

Urban coastal flood prediction: Integrating wave overtopping, flood defenses and drainage



T.W. Gallien^{a,b}, B.F. Sanders^{a,*}, R.E. Flick^c

^a Department of Civil and Environmental Engineering, University of California, Irvine, United States

^b Scripps Institution of Oceanography, University of California, San Diego, United States

^c Department of Boating and Waterways, Scripps Institution of Oceanography, University of California, San Diego, United States

ARTICLE INFO

Article history:

Received 17 January 2013

Received in revised form 18 April 2014

Accepted 22 April 2014

Available online 2 June 2014

Keywords:

Coastal flooding

Overtopping

Flood mapping

Urban flooding

Berm

Urban drainage

ABSTRACT

Flood extent field observations collected following a wave overtopping event are used to evaluate the accuracy of two urban flood prediction models: a static ('bathtub') model that simply compares water level to land elevation, and a hydrodynamic model that resolves embayment dynamics, overland flow, concrete flood walls, and drainage into the storm water system. Time-dependent overtopping rates were estimated using empirical models parameterized with survey data and local wave heights transformed to the nearshore using Simulating Waves Nearshore (SWAN) and subsequently input to the hydrodynamic model. The hydrodynamic model showed good agreement with field observations, whereas the static model substantially overpredicted flooding suggesting that urban backshore flood depths do not equilibrate with shoreline water levels in transient events. In the absence of a high backwater condition, storm system drainage attenuates wave overtopping flooding. Hydrodynamic model simulations suggest that bay side flood defenses may exacerbate flooding by restricting drainage and that temporary flood mitigation berms can significantly reduce backshore flooding. This study points to a promising urban coastal flood prediction and management framework.

© 2014 Elsevier B.V. All rights reserved.

1. Introduction

Newport Beach, California is a highly urbanized low-lying coastal community with large portions of the city below extreme high tide levels. With numerous such lowlands across the State, over 325,000 people live within 1 m of local mean high water levels (Strauss et al., 2012). Globally sea levels are expected to rise on the order of 0.5–1 m by 2100 (Church et al., 2013), and in California, the State is recommending that coastal communities plan for 26–43 cm of sea level rise (SLR) by 2050 and for 110–176 cm by 2100, under the assumption of a high greenhouse gas emission scenario (State of California, 2010). Framed in the context of coastal flood frequency, an alarming result emerges that approximately four decades of SLR will transform the present day 100 year coastal flooding event in Southern California into an annual occurrence (Tebaldi et al., 2012). Effective risk management will require advanced coastal flooding models responsive to dynamic changes in water levels, wave forcing, and infrastructure (National Research Council, 2009).

Urban coastal flood prediction presents numerous challenges: complex forcing mechanisms (variability of ocean levels, waves and rainfall), geometrical complexities of urban environments (flood walls, buildings, drainage systems), nonlinear feedbacks associated with

natural processes (e.g., beach erosion), and human decision-making (e.g., sandbagging, operation of drainage infrastructure, berming). A general framework has been established around two-dimensional (2D) hydrodynamic models that simulate overland flow (e.g., Bates et al., 2005; Brown et al., 2007; Dawson et al., 2009; Knowles, 2009; Martinelli et al., 2010; Purvis et al., 2008; Smith et al., 2012; Villatoro et al., 2014; Wadey et al., 2012); however, individual component implementations such as flow routing, flood defense representation, boundary conditions, and wave overtopping volumes differ.

Overland flow may be routed via simplistic static (bathtub) projections (e.g., Heberger et al., 2009), mass conservation schemes (e.g., LISFLOOD) (Bates and De Roo, 2000) or hydrodynamic models based on the shallow-water equations (e.g., TUFLOW, DIVAST, BreZo). Poulter and Halpin (2008), Heberger et al. (2009) and Strauss et al. (2012) present raster-based flood models where areas that fall below the water level are flooded, i.e., the models assume that flow paths exist and the flood is sustained sufficiently long to fill the impacted region to the height of the embayment. The static method, also known planar surface projection or equilibrium method, has drawn criticism for poor predictive skill (Bernatchez et al., 2011; Gallien et al., 2011). Variants of this approach can be devised to account for protection by levees and seawalls, but all static models retain the assumption that flooding occurs instantaneously upon exceeding the overtopping threshold. Protective barrier failure can be integrated into static and hydrodynamic models (e.g., Brown et al., 2007), but only the hydrodynamic approach accounts for temporal effects.

* Corresponding author.

E-mail addresses: tgallien@ucsd.edu (T.W. Gallien), bsanders@uci.edu (B.F. Sanders), rflick@ucsd.edu (R.E. Flick).

Numerous studies have suggested complex features such as curbs, walls, berms and localized sources and sinks need to be included in urban flood models (e.g., Bernatchez et al., 2011; Brown et al., 2007; Fewtrell et al., 2008; Gallegos et al., 2009; Gallien et al., 2011; Mignot et al., 2006; Poulter and Halpin, 2008). Néelz et al. (2006) found that LiDAR data inadequately resolved hydraulically important features such as walls and embankments. Similarly, Webster et al. (2004) showed that abrupt elevation changes typical of wharves, flood defense walls, and cliffs are inadequately resolved for inundation modeling. More recent studies have begun to explicitly represent flood defenses. For example, Poulter and Halpin (2008) elevated individual raster pixels to include flood defenses while Smith et al. (2012) elevated individual digital elevation model (DEM) cells for input into a hydraulic flood model. Alternatively, Gallien et al. (2011) carefully aligned a computational mesh used by the hydrodynamic model to depict flood defense walls. Temporary flood management practices such as cautionary sand bagging and beach berming are often sub-LiDAR scale and because of their temporary nature, may not be deployed during the LiDAR data collection.

Hydrodynamic model boundary conditions account for dynamic sea level changes corresponding to hourly and longer time scales such as tides and storm surge. Approaches for boundary conditions include synthetic time series representative of extreme high tides (e.g., a 100 year event), output from multi-scale models and historical data. These dynamic approaches contrast with simplistic sea level rise assessments that utilize a static water level value depicting a future sea level (e.g., Coveney and Fotheringham, 2011; Gesch, 2009; Kirshen et al., 2008; Strauss et al., 2012; Yin et al., 2011). Brown et al. (2007) present a coupled storm surge and overland flow model for Canvey Island located in the Thames Estuary. Similarly, Knowles (2009) established a San Francisco Bay model domain that was externally forced at the Golden Gate by a water level time series that accounts for total ocean height, a combination of tidal and non-tidal (e.g., storm surge, atmospheric pressure changes) factors, as well as inland streamflow. Smith et al. (2012) used historical tide gauge records to estimate local water levels in an area along the Bristol Channel. Alternatively, Martinelli et al. (2010) developed probabilistic water levels at the shoreline of Emilia Romagna along the Adriatic Sea in Northern Italy to force an overland flow model.

Overtopping flows represent a critical component of coastal flood mapping; however, dynamic wave overtopping volumes are rarely included in coastal flood predictions. Accordingly, methods considering wave overtopping have been recognized as a research priority (Wadey et al., 2012). A simplistic method for depicting overtopping flooding involves adding maximum wave runup to determine a total water level (e.g., FEMA, 2004; Heberger et al., 2009) and projecting this water level across the land surface. The total water level method is applied using a static model and consequently suffers identical deficiencies: hydraulic connectivity may not be enforced, and offshore water levels may not be sustained sufficiently long for backshore water levels to equilibrate. Overtopping time scales in episodic flooding events caused by coincident large wave conditions and high tides range from minutes to a few hours, which is insufficient time to fill the backshore. Total water level wave overtopping estimates have proven to significantly overpredict flooding zones (Bates et al., 2005; Gallien et al., 2013).

Only a limited number of studies include temporally variable overtopping estimates (Cheung et al., 2003; Chini and Stansby, 2012; Laudier et al., 2011; Lynett et al., 2010; Martinelli et al., 2010). Numerical models represent the current state-of-the-art for simulating overtopping flows and theoretically, if the physics are well represented, could predict overtopping in an infinite number of dune, dike, or wall configurations. However, field-scale implementations have been challenged by computational effort and sensitivities to grid spacing and boundary conditions that restrict most applications to numerical wave flumes (e.g., Hu et al., 2000) or analytical solutions and laboratory validation data

(e.g., Hubbard and Dodd, 2002; Liu et al., 1999; Losada et al., 2008; Okayasu et al., 2005). Empirical simple-slope overtopping models, on the other hand, are widely used mature methods benefiting from extensive research (e.g., Owen, 1980; USACE, 1984; Ahrens et al., 1986; Hedges and Reis, 1998; TAW, 2002; Mase et al., 2003; Pullen et al., 2007; Reis et al., 2008).

Few studies have attempted to validate flooding from wave overtopping. Field observations on a central California beach suggest that empirical models moderately overestimate overtopping rates (Laudier et al., 2011). Cheung et al. (2003) and Lynett et al. (2010) presented numerical overtopping models along with qualitative validation data (e.g., high water marks or levee damage) and in the case of Lynett et al. (2010), empirical and numerical estimates differed by a factor of 10. Smith et al. (2012) considered an urban coastal flood event along the North Somerset coast in the UK and used point sources to introduce overtopping volumes to the flooding domain, however overtopping rates were not modeled in a prognostic manner, but rather from a post event analysis of the flooded area that revealed flood volume. Moreover, the analysis suggested significant uncertainty in the overtopping estimate, and the study concluded that overtopping volumes are a dominant source of uncertainty relative to flood extent prediction. Indeed, wave overtopping is considered a significant deficiency in the current modeling methodology (Brown et al., 2007; Hubbard and Dodd, 2002; Hunt, 2005), and multiple studies stress the need for field validation data (Anselme et al., 2011; Battjes and Gerritsen, 2002; Gallien et al., 2013; Poulter and Halpin, 2008; Reeve et al., 2008; Thomalla et al., 2002).

This paper presents an integrated hydrodynamic flood model that accounts for the combined effects of overland flow, flood defenses, dynamic sea level changes, temporally variable wave overtopping volumes and urban drainage. Static and hydrodynamic model outcomes are compared with flood extent field observations at a California site. Finally, hydrodynamic model simulations investigate the impacts of anthropogenic beach berming and the implications of fortified bay side flood defense walls on wave overtopping floods.

2. Methods and materials

2.1. Newport Beach site description

Newport Beach, California, Fig. 1, is located approximately 70 km southeast of Los Angeles. The City of Newport Beach encompasses Newport Harbor and is geographically characterized by elevated marine terraces and the urban coastal lowlands of Balboa Peninsula and the constructed islands within Newport Harbor. Balboa Peninsula is exposed to two modes of flooding: (1) weir-like overtopping of low-profile (<50 cm high) concrete flood walls on the bay side of the Peninsula, as shown in Fig. 2a, and (2) wave overtopping of its ocean facing beaches which are exposed to high wave energy, particularly its south-facing beaches (south of Newport Pier), as shown in Fig. 2b. These processes may or may not be concurrently active, and ironically, in the present case, flooding may be exacerbated by embayment flood defenses.

The Balboa Peninsula storm water system is gravity drained into the harbor and tide valves are installed at each outfall. The Peninsula has a long history of episodic flooding that is proactively managed by the City of Newport Beach. Tide valves are manually operated according to water levels to prevent back flooding, and elevated sand berms are constructed in advance of major swell events to protect against wave overtopping (Schubert et al., *in press*). On August 31, 2011 a long-period southern swell arrived approximately 12 h earlier than forecast, and prior to protective berm construction. This resulted in beach overtopping near Balboa Pier and flash flooding of the urban backshore. This event provides a unique field opportunity to investigate an integrated prognostic flood modeling methodology.

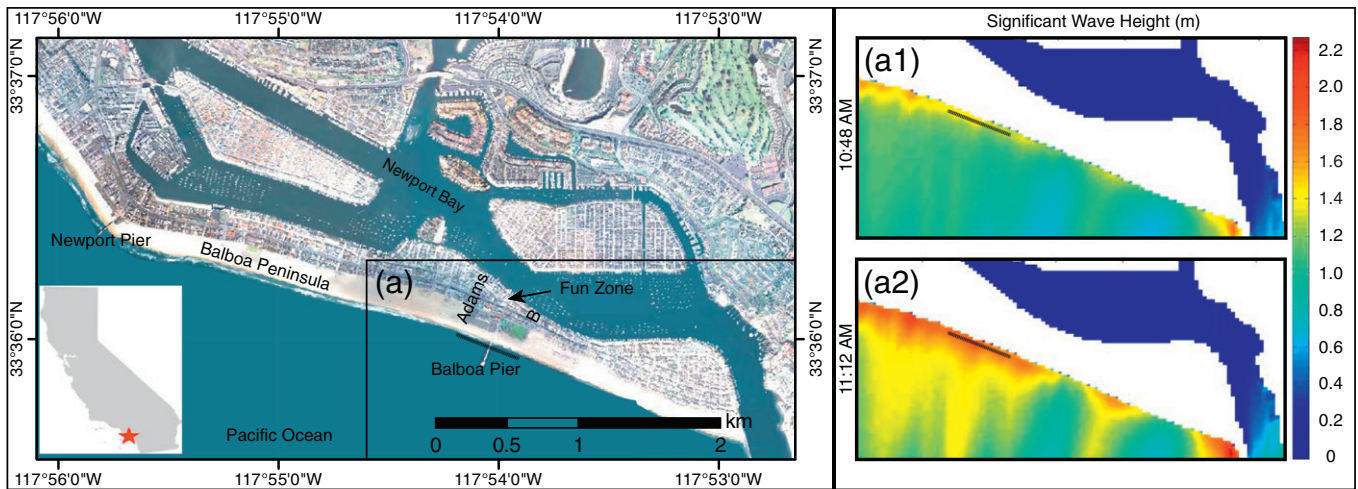


Fig. 1. Newport Beach, California. Insets show wave height details at (a1) 10:48 AM and (a2) 11:12 AM, during peak overtopping. The dashed line represents the location over which wave heights were averaged for overtopping calculations.

2.2. Site data

A bare earth digital terrain model (DTM) in NAD83 and NAVD88 consisting of all topography and bathymetry within the simulation domain was prepared from LiDAR and bathymetry data. The City of Newport Beach provided orthoimagery and LiDAR from a 2006 city-commissioned survey. Orthoimagery originally supplied at approximately 8 cm resolution was later coarsened to 30 cm to facilitate data management. The final LiDAR data consisted of over 10 million irregularly spaced bare-earth samples with a vertical accuracy of 0.182 m (RMSE). Upper and Lower Newport Bay bathymetry was obtained from two U.S. Army Corps of Engineering surveys with 1 and 3 m resolutions and vertical accuracies of ~ 0.1 m. Three arc-second horizontal resolution offshore bathymetry was retrieved from the Southern California Coastal Ocean Observing System (SCCOOS). LiDAR survey returns on critical flood defense structures (e.g., concrete sea walls and high embankments) were minimal; therefore publicly accessible barrier elevations were surveyed using a Real Time Kinematic (RTK) survey with vertical RMSE of 1–2 cm (Gallien et al., 2011). All data were merged into a single point file consisting of over 12 million points and interpolated to create a 3 m resolution DTM.

In addition to the city LiDAR survey, six Scripps Southern California Beach Process LiDAR datasets (SCBPS, 2014), and an RTK survey, shown in Table 1 were used to characterize the beach face. Vertical accuracy of the Scripps LiDAR is 10 cm vertical RMSE (SCBPS, 2014).

2.3. Validation data event description

On August 31, 2011 a large southern swell event generated by an Antarctic low pressure system arrived earlier than forecast and

coincided with a high tide at 11:20 AM of 1.81 m NAVD88. Individual waves ran up and overtopped the beach near Balboa Pier from approximately 11:00 AM to 12:00 Noon PDT causing localized flooding from B Street west to Adams Street. City service employees reported that all storm drains were open at the time of overtopping with the exception of A and B streets. On September 1 wrack lines were mapped on high resolution satellite photos. In areas where clear wrack lines were absent, residents were interviewed and observations were supplemented by city service worker photographs and media coverage (e.g., CBS, 2011 Los Angeles Times, YouTube and Patman Films). The flood zone was digitized as a polygon layer in ArcMAP.

2.4. Local wave climate

Deep water spectral data were retrieved from CDIP buoy 096 located approximately 20 km southeast of the site off the coast of Dana Point, California and transformed using SWAN (Simulating WAVes Near-shore), a third generation numerical wave model (Booij et al., 1999). Hourly frequency directional spectra in 360 directional and 64 frequency bins were calculated using the maximum entropy method and applied as the deep water boundary condition approximately 10 km offshore in ~ 450 m water depth. A regular simulation domain of 11×10 km with a grid resolution of $28 \text{ m} \times 22 \text{ m}$ was carefully chosen through an iterative process to ensure that east and west boundary locations and grid spacing did not affect simulation outcomes. A total of 24 simulations in two dimensional stationary mode were run, wave spectra were updated hourly and water levels every 30 min. Fig. 1 shows the spatial variability of significant wave height before (inset a1) and during (inset a2) overtopping. Fig. 3a shows a time series of longshore averaged significant wave heights at the slope toe, ~ 0 MLLW, for overtopping model input.



Fig. 2. Overtopping in Newport Beach, California.

Table 1
Beach face summary statistics.

Data	Year	Month	\bar{z} (m)	σ (m)	z_{max} (m)	$1/\beta$	σ
Scripps	2009	March	4.91	0.073	5.24	7.56	0.43
Scripps	2008	October	4.85	0.070	5.31	7.40	0.41
Scripps	2007	April	5.03	0.125	5.35	7.25	0.58
Scripps	2006	October	4.94	0.168	5.41	7.31	0.42
Scripps	2004	March	4.89	0.070	5.43	7.89	0.58
Scripps	2004	September	4.91	0.073	5.44	7.76	0.51
UCI	2006	April	4.90	0.149	5.14	8.05	0.75
All Lidar	–	–	4.92	0.107	5.44	7.60	0.59
Survey	2012	May	5.02	0.162	5.38	–	–

2.5. Static flood modeling

Static flood modeling is a simple alternative to hydrodynamic modeling for coastal flood mapping and relies upon a comparison of water level to ground elevation. The assumption is that land below the ocean level is flooded instantly. Two ocean water levels are considered to map flood zones: observed water level (OWL) and total water level (TWL). The former projects the observed maximum tide elevation and the latter includes a maximum runup elevation estimated using Stockdon et al. (2006),

$$R_{2\%} = 1.1 \left(0.35\beta(H_0L_0)^{0.5} + \frac{[H_0L_0(0.563\beta^2 + 0.004)]^{0.5}}{2} \right) \quad (1)$$

where H_0 is the deep water significant wave height, L_0 is the deep water wave length and β is the foreshore beach slope.

2.6. Hydrodynamic flood modeling

Two-dimensional Godunov-type finite volume models based on the nonlinear shallow water equations are relatively new to flood modeling but have been shown to support an accurate and stable prediction of flooding and drainage dynamics (e.g., Hubbard and Dodd, 2002; Sanders, 2008). Godunov-type schemes rely on an approximate Riemann solver to compute mass and momentum fluxes along the edges separating neighboring computational cells (Guinot, 2003; Toro, 2001), and admit a wide range of flow regimes including supercritical flows from abrupt elevation changes inherent to urban environment such as flood defenses, streets, and curbs without case specific parameter tuning. Godunov-type finite volume codes have been successfully implemented in coastal embayment modeling (Arega and Sanders, 2004; Cea et al., 2006; Gallien et al., 2011; Sanders, 2008) and urban flood simulation (Gallegos et al., 2009; Mignot et al., 2006; Sanders, 2008; Schubert and Sanders, 2012; Schubert et al., 2008; Villaneueva and Wright, 2006), thus representing an attractive basis for integrated embayment flooding events, i.e., resolving embayment long-wave dynamics, weir-like overtopping, and overland flow into low lying terrain.

BreZo (Begnudelli et al., 2008; Sanders, 2008), applied here, uses an unstructured computational mesh defined by a constrained Delaunay triangulation. The simulation domain requires approximately 500,000 cells to represent all above and under water terrain near Newport Bay and extends several kilometers offshore. The mesh was generated using Triangle (Shewchuk, 1996). A minimum angle constraint of 30° eliminates stability problems that occur with highly acute angles. Spatially variable area constraints focus computational resources on the urbanized lowlands (ca. 3.5 m horizontal resolution). Cell sizes were gradually coarsened in areas of increasing ocean depth or high elevation (ca. 300 m). Edge constraints were implemented to align mesh

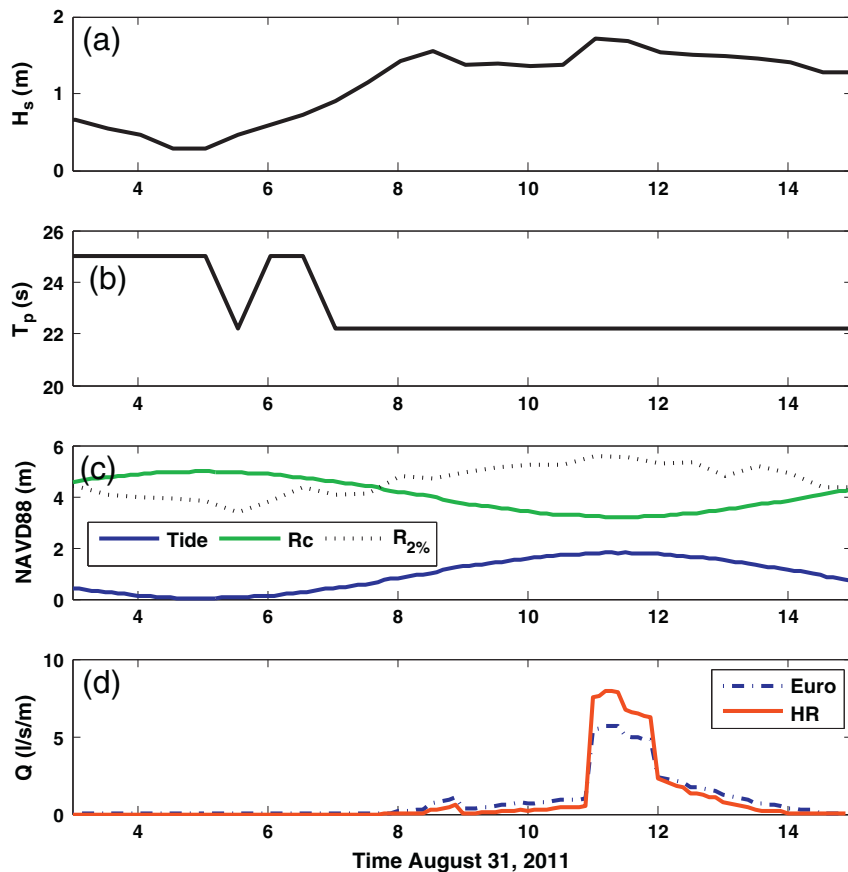


Fig. 3. Time series of (a) significant wave height at the slope top (H_s), (b) peak period (T_p), (c) tide level (blue), freeboard (green), Stockdon $R_{2\%}$ (dashed) and (d) overtopping estimates.

edges with land surface features subject to overtopping. Critically, mesh edge alignment facilitates highly accurate surveyed flood defense wall elevations (ca. 1 cm) to be implemented within the hydrodynamic model (Gallien et al., 2011).

Six minute water levels for August 31, 2011 were obtained from the nearest tide gauge located approximately 40 km to the northwest in the port of Los Angeles (NOAA, 2012) and applied as the offshore boundary condition for BreZo. The simulation starts approximately 8 h before the peak tide and resolves the ebb–flood–ebb cycle (3:00 AM to 15:00 PDT) that captures the minor tidal amplification observed within Newport Bay. The Godunov model solves a Riemann problem and therefore handles any weir-like wall overtopping for flood defenses on the bay side. Overtopping volumes and drainage outflows are integrated into the hydrodynamic model using point sinks and sources as detailed in the following sections.

2.6.1. Urban drainage models

Curb inlets are modeled as point sinks. The volumetric flow rate is based on a broad crested weir equation (Sturm, 2001),

$$Q = \frac{2}{3} C_v C_d \left(\frac{2}{3} g \right)^{1/2} L H^3 \quad (2)$$

where Q represents flow into the storm system, L is the width of the drain opening and H is the water depth and, in this case, the product of C_v and C_d is equal to unity (Orange County Environmental Management Agency, 1996). Eq. (2) is valid for water depths less than or equal to the inlet height. After water depth exceeds two times the inlet height the orifice equation is used (Sturm, 2001),

$$Q = C_d A (2gH')^{1/2} \quad (3)$$

where A is the area of the inlet, H' is the head acting on the center line of the inlet and C_d is 0.70 (Orange County Environmental Management Agency, 1996). Flows for water levels between one and two times the inlet height may be estimated using a nomograph (Orange County Environmental Management Agency, 1996).

Tide elevation during the August 31, 2011 event was well below the threshold for tide valve closure (2.08 m NAVD88). Point sinks within the hydrodynamic model represent each of the 14 curb inlets (Fig. 6). Flows are computed using Eq. (2). The sink rate was simply modeled and assumed to withdraw a constant flow where the water level was equal to drain inlet height, although this assumption overestimates fluid withdrawal during low flow, it is a reasonable approximation near peak overtopping levels since maximum water elevations are similar in magnitude to inlet heights.

2.6.2. Wave overtopping models

Runup and overtopping volumes typically infiltrate into the wide sandy beach, however adjacent to Balboa Pier, the beach is comparatively narrow (<50 m) and impermeable areas (parking lots and roads) collect and transfer overwash to the urban backshore. Temporally variable wave overtopping volumes are estimated using two empirical overtopping models: Hedges and Reis (Hedges and Reis, 1998; Reis et al., 2008) and Eurotop (Pullen et al., 2007) abbreviated hereafter as HR and Eurotop, respectively. Simple-slope overtopping models are well documented and geometrically consistent with the beach dune system in Newport Beach, therefore representing an attractive candidate for estimating overtopping rates. Although the empirical models were originally intended for runup and overtopping of structures, they have been employed in beach and dune overtopping studies (e.g., Laudier et al., 2011; Martinelli et al., 2010).

The probabilistic Eurotop formulation, where 50% of empirical data points are not exceeded and $\xi_{m-1,0} < 5$ is,

$$\frac{q}{\sqrt{gH_{m0}^3}} = \min(a, b)$$

$$a = \frac{0.067}{\sqrt{\tan\alpha}} \gamma_b \xi_{m-1,0} \exp\left(-4.75 \frac{R_c}{\xi_{m-1,0} H_{m0} \gamma_b \gamma_f \gamma_\beta \gamma_v}\right) \quad (4)$$

$$b = 0.2 \exp\left(-2.6 \frac{R_c}{H_{m0} \gamma_f \gamma_\beta}\right)$$

where H_{m0} is the significant wave height at the toe of the structure, R_c is the freeboard, α is the angle of the slope, g represents gravity, q is the mean overtopping rate per unit length, γ_b is the berm influence factor, γ_f is the roughness influence factor, γ_β is the oblique wave attack factor and γ_v is the vertical wall influence factor (Pullen et al., 2007). All reduction parameters were assumed to be unity: no subaerial berm was present, the sand was saturated and assumed to be smooth and impermeable, peak wave direction was within a few degrees of orthogonality and no vertical wall was present at the beach crest. The TAW (2002) formulation relies on a breaker parameter $\xi_{m-1,0}$ that characterizes the wave breaking condition (i.e., breaking, non-breaking) and is given as,

$$\xi_{m-1,0} = \frac{\tan\alpha}{\sqrt{\frac{H_{m0}}{L_{m-1,0}}}} \quad (5)$$

where $L_{m-1,0}$ is the deep water wave length (Pullen et al., 2007).

Similarly, the HR irregular wave overtopping model (Reis et al., 2008) is

$$\frac{q}{\sqrt{gR_{max}^3}} = \begin{cases} A \left(1 - \frac{R_c}{\gamma_r R_{max}}\right)^B & \text{for } 0 \leq \frac{R_c}{\gamma_r R_{max}} < 1 \\ 0 & \text{for } \frac{R_c}{\gamma_r R_{max}} \geq 1 \end{cases} \quad (6)$$

where γ_r is a roughness parameter and A and B are described by

$$A = \begin{cases} 0.0033 + 0.0025 \cot\alpha & \text{for } 1 \leq \cot\alpha \leq 12 \\ 0.0333 & \text{for } 12 < \cot\alpha \leq 20 \end{cases} \quad (7)$$

and

$$B = \begin{cases} 2.8 + 0.65 \cot\alpha & \text{for } 1 \leq \cot\alpha \leq 8 \\ 10.2 - 0.275 \cot\alpha & \text{for } 8 < \cot\alpha \leq 20 \end{cases} \quad (8)$$

where R_{max} is the maximum expected runup using the Mase et al. (2003) extension of Hunt's (1959) equation that incorporates wave set up,

$$\frac{R_{max}}{H_s} = \begin{cases} 0.38 + 1.67 \xi_p & \text{for } 0 < \xi_p \leq 2.2 \\ 4.56 - 0.23 \xi_p & \text{for } 2.2 < \xi_p \leq 9.0 \\ 2.51 & \text{for } 9.0 < \xi_p \end{cases} \quad (9)$$

and ξ_p is the surf similarity parameter,

$$\xi_p = \frac{\tan\alpha}{\sqrt{\frac{H_s}{L_0}}} \quad (10)$$

where H_s is the significant wave height measured at the toe of the slope and L_0 is the deep water wave length, $L_0 = gT_p^2/2\pi$.

2.6.3. Overtopping model parameterization

The empirical overtopping models are parameterized using nearby CDIP wave buoy (096) spectra transformed to the nearshore (Fig. 1) and a mix of survey, geospatial and tide data. Eurotop and HR require an intermediate surf similarity parameter calculation however, the recommended parametrization varies slightly. HR relies upon the peak

period whereas Eurotop employs spectral period. For a narrow banded spectrum, $T_p \approx 1.1 T_{m0}$ (Pullen et al., 2007). Balboa beach profiles, Fig. 4, and a prior USACE study (USACE, 2002) show a distinct transition from a shallow nearshore slope (~1:20) to a steeper foreshore (~1:8) occurring near 0 m MLLW (-0.04 m NAVD88). This slope break is evident in recovered season profiles (Fig. 4 – solid lines, arrows) consistent with the late August event and, for the purpose of this work, is considered the slope toe.

Freeboard is the difference between the maximum beach crest elevation and the tide elevation and was estimated using LiDAR data and a walking survey. LiDAR sampling of the beach often underestimates maximum beach crest elevation, the highest cross shore elevation may not have produced LiDAR returns and the sampling strategy may include adjacent LiDAR points that slightly depress elevation statistics. Seven LiDAR datasets were examined to determine the possible range of values for beach crest elevation and slope. Generally the average crest elevation for all LiDAR data was similar, ranging from 4.85 to 5.03 m and is shown in Table 1. Maximum elevation for all LiDAR surveys was 5.37 m and the RTK survey maximum elevation was 5.38 m. Since the maximum crest elevation appears to be consistent throughout the LiDAR data and the RTK survey guarantees maximum crest height, the RTK crest elevation of 5.02 m was used to calculate freeboard. Beach profiles corresponding to seasonal recovery, September and October LIDAR data, are used to estimate a beach slope of 1:7.5.

Six minute water levels, beach geometry data, and SWAN significant wave height estimates at the slope toe were used to evaluate freeboard and calculate a time series of empirical overtopping estimates (Fig. 3d) as input of the hydrodynamic model. The overtopping flow rate is updated every six minutes in accordance with the tide measurements, and assumed constant for the period between tide measurements. Wave overtopping volumes are introduced to the model slightly landward of berm crest (Fig. 6) and BreZo hydrodynamically routes all overland flow volumes.

2.7. Fit measures

Model skill may be assessed using three fit metrics that consider the agreement between predicted and observed flood extents. An agreement fit measure, F_A , is the coefficient of areal correspondence (Taylor, 1977), and represents the intersection of predicted and observed flood extents divided by the union of the predicted and observed flood extent,

$$F_A = \frac{E_p \cap E_o}{E_p \cup E_o} \tag{11}$$

where E_o and E_p are the observed and predicted flood extents. F_A of zero and unity correspond to no agreement and complete agreement,

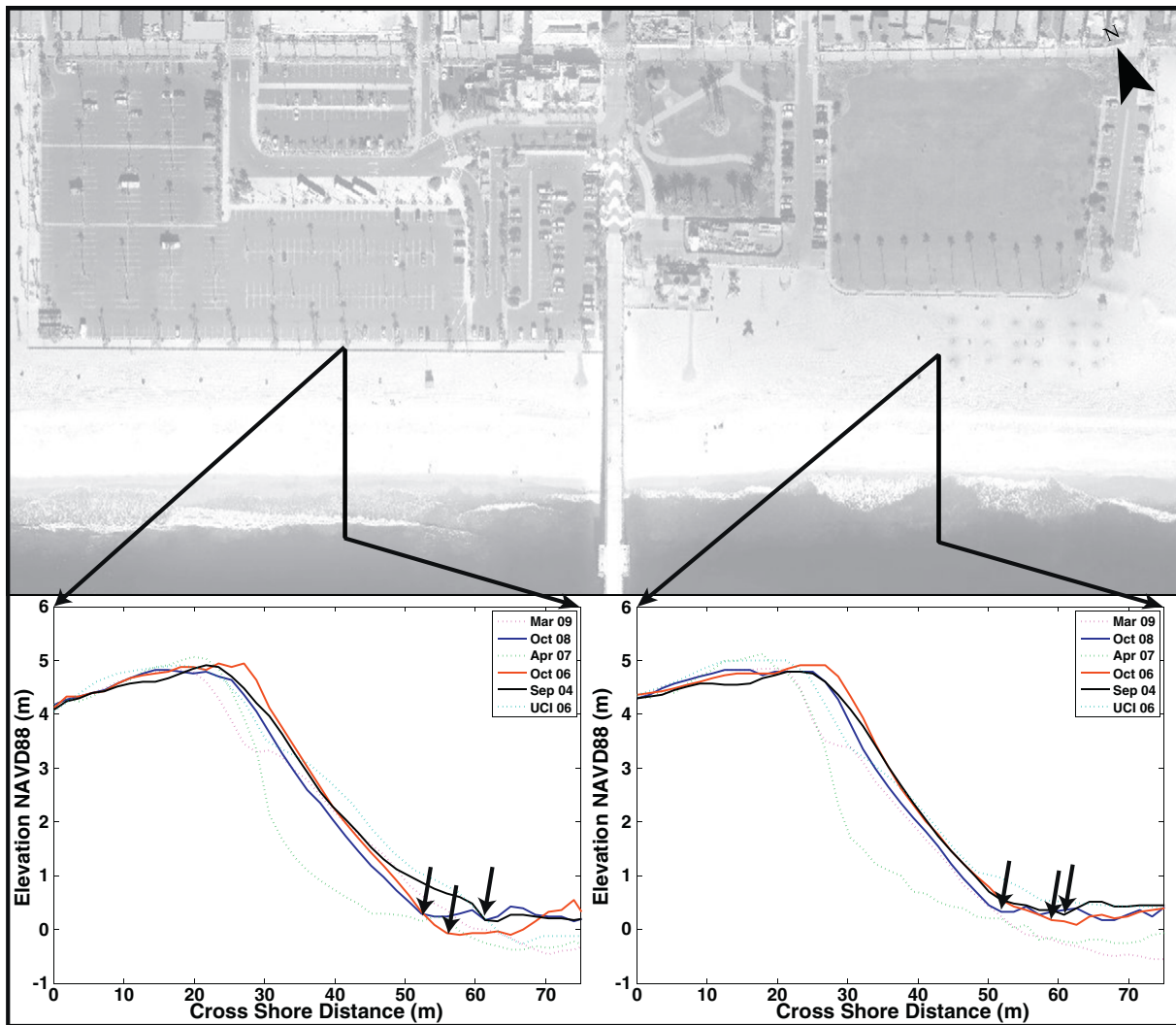


Fig. 4. Representative transects at Balboa Beach. Summer and fall (recovered) profiles are shown as solid lines, approximate slope toes are marked with arrows. Winter and spring (eroded) season profiles are shown as dashed lines.

Table 2
Static and hydrodynamic flood predictions.

Figure	Model	A (km ²)	F _A	F _{UP}	F _{OP}
–	Static OWL	–	–	1.00	–
5a	Static TWL (R _{2%})	2.14	0.02	–	0.98
5b	Hydro w/Eurotop	0.08	0.36	0.06	0.58
5c	Hydro w/HR	0.09	0.36	0.03	0.61

respectively. A measure of underprediction, F_{UP} , characterizes the fraction of flooded area observed, but not predicted as follows,

$$F_{UP} = \frac{E_O - E_P \cap E_O}{E_P \cup E_O} \quad (12)$$

and $F_{UP} = 0,1$ correspond to no underprediction and complete underprediction, respectively. Lastly, a measure of overprediction, F_{OP} , characterizes the fraction of flooded area predicted but not observed as follows,

$$F_{OP} = \frac{E_P - E_P \cap E_O}{E_P \cup E_O} \quad (13)$$

where $F_{OP} = 0,1$ correspond to no overprediction and complete overprediction, respectively. Superior models will maximize F_A while minimizing both F_{UP} and F_{OP} .

3. Results

3.1. Static and hydrodynamic predictions

Modeling was performed on a personal computer with an Intel quad core 3.6 GHz processor. Static model implementation in GIS is nearly instantaneous. Hydrodynamic model simulation time resolving an ~12 hour tide cycle utilizing a 0.05 s times step required approximately seven hours of wall clock time. In this case, the hydrodynamic solver was run in a serial configuration (single core) however, parallel processing would support larger domains while preserving reasonable simulation times.

All firsthand reports of the August 2011 event suggested that flooding was exclusively driven by wave overtopping from the ocean side near Balboa Pier. For further verification, the model was initially

applied assuming no wave overtopping to consider the possibility of flooding from weir-like overflow caused by high embayment water levels. No flooding was predicted. The maximum predicted embayment water level was 1.83 m, well below the ca. 2.2 m NAVD88 threshold of bay side wall overtopping (Gallien et al., 2011).

Table 2 and Fig. 5 show static and hydrodynamic flood prediction results. The static method employing either an offshore water level of 1.81 m NAVD88 level predicts no flooding while a Stockdon R_{2%} total water level of 5.58 m floods the entire peninsula (Fig. 5a). Static model fit statistics (Table 2) reflect poor static model skill, TWL results in total over prediction and areal extent differs by two orders of magnitude from the observed flood.

All following models represent an integrated process description that includes tide, tidal amplification within the embayment, drainage representation, temporally variable wave overtopping volumes and overland flow across urban terrain. The hydrodynamic methods significantly improve flood predictions relative to the static methods (Fig. 5b, c), F_A drastically increases, underprediction is nearly zero and overprediction is moderate. Eurotop and HR predict similar flooded area, 0.08 and 0.09 km², respectively. HR predicts a larger areal extent (most visible on the west edge of the domain) and slightly enhanced water depths (Fig. 5c) consistent with higher overtopping estimates (Fig. 3d).

3.2. Urban drainage and flood defense structures

Three simulations highlight the effects of drainage (Fig. 6, Table 3), when drainage is omitted (blue) the flood prediction is large, 0.105 km², overprediction dominates, $F_{OP} \sim 0.7$, flood depths are the highest of the study, $h_{avg} = 14.6$ cm and depth at the street end (h_{se}) is large, 102 cm. Adding drainage improves model skill, reduces average flood depth and decreases flood prediction area to ~0.8 km². When drains A and B are closed (as reported) the flooded area increases approximately 9% (purple in Fig. 6).

The hydrodynamic model's computational mesh is prepared with edges aligned with flood walls so that wall heights may be explicitly specified. Table 3 shows the consequence of the flood defense wall on the bay side of the peninsula. Removal of the wall from the flood model reduces flood extent by 15% and predicts the lowest average flood depth (9 cm). Instead of spreading out, flood waters flux directly into the bay. If the wall is raised to 30 cm, to protect against weir-like flooding from the bay side, the average flood depth increases to 12.2 cm. No change in the area is noted from the original prediction,

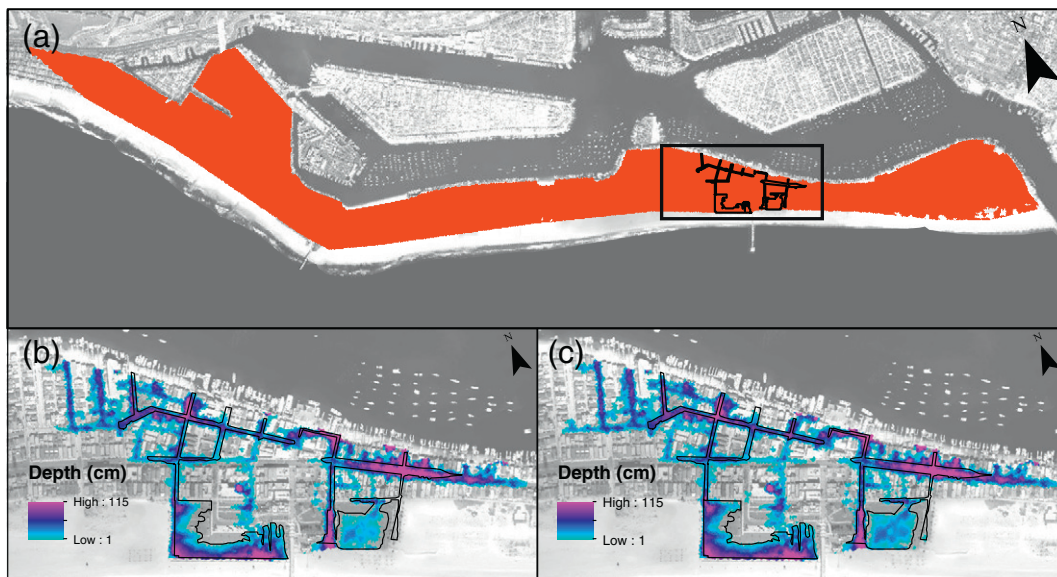


Fig. 5. Static (a) and hydrodynamic (insets b & c) results with Eurotop and HR overtopping estimates, respectively. The black outline represents the observed flood extent.

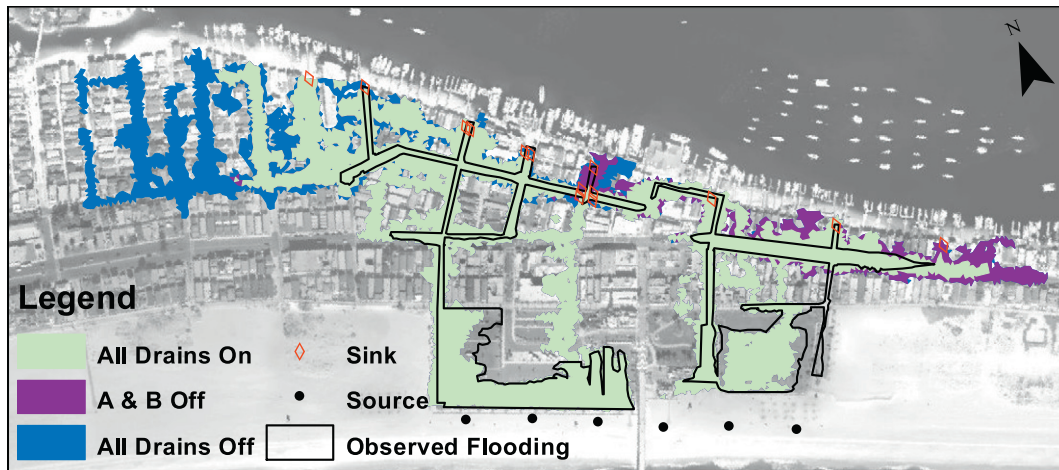


Fig. 6. Drainage results. Source and sink locations are shown as open diamonds and closed circles, respectively. Light shading is the flood prediction with all drains depicted as on. The purple shading shows additional fractional areas flooded when A and B drains are off. Blue represents additional area predicted to flood if all drains are inoperable. The black outline is the observed flood.

however the flood is significantly scaled by the wall elevation in larger volumetric overtopping events. For example, Fig. 7 shows flood predictions for an identical event with 30 cm of additional wave elevation consistent with a typical Perigean spring tide or strong El Niño event. Average depth increases ~20%, low-lying street end depth doubles and areal extent increases ~35% to 0.12 km². These results show that an elevated wall would increase ponding caused by wave overtopping and that flood defense walls protecting peninsulas or barrier islands against high embayment water levels can exacerbate flooding caused by waves overtopping ocean beaches.

Similar wave and tide conditions persisted for approximately 24 h after the flood event. On September 1st, 2011 the day following the flood, the observed high tide level at Los Angeles was 4 cm above the previous day’s high tide and wave conditions were similar, however, no backshore flooding except for small areas immediately adjacent to the berm was observed. This is attributed to the construction of a temporary sand berm by the City of Newport Beach (Fig. 2c). Field observations in this study suggest that berms play a key role in protecting the urbanized backshore in transient events.

Fig. 8 shows the results of a berm added to the August 31 simulation. The addition of the berm to the simulation resulted in 73% decrease in predicted flood area to 0.02 km². These findings highlight two key results, resolving temporary flood abatement measures (e.g., berms or sand bagging) significantly affects flood predictions and, in this case, empirical models overestimate overtopping volumes.

4. Discussion

Runup and overtopping volumes are central to flood mapping efforts. Simple static methods inadequately predict transient flooding events and represent extreme flood predictions, complete under- or overprediction; no flooding was predicted using an offshore water level, conversely a TWL projection using Stockdon R_{2%} flooded the entire peninsula. Although static models have proven useful in raising awareness about the long term impacts of sea level rise (e.g., Heberger et al., 2009; Strauss et al., 2012), ultimately these models undermine flood risk management efforts to identify optimal resource allocation. The empirical overtopping model coupling presented here moderately overestimates wave overtopping volumes however, it represents substantial improvement over static mapping methods, flood predictions are same order of magnitude, spatial distribution is consistent with observation and the time of overtopping vulnerability (11:00 AM–12:00 PM) is accurately predicted. The modeling framework presented here incorporates the appropriate sensitivities for meaningful coastal flood risk

projections. This includes a sensitivity to higher high tides, waves, changes to flood defenses including beaches and flood walls, and inclusion of drainage infrastructure.

Urban drainage is critical to predicting the extent and depth of transient overtopping floods. Gallien et al. (2011) also show that the storm drain system may act to redistribute flood water even when the outlets are closed to prevent back-flooding from high embayment levels. That is, water entering one curb inlet may cause surging in another resulting in isolated pools on the land surface. These pools cannot be predicted by models which ignore drainage, a finding that challenges the assumption of recent studies of urban flooding that storm system flows can be ignored when the drainage system is operating at capacity (e.g., Fewtrell et al., 2011; Sampson et al., 2012). Furthermore, recognizing that City of Newport Beach personnel close outfalls to prevent back flooding during high tide events, surface water removal through the drainage system is limited by the storage capacity of the underground pipes. These findings point to increased flood risk with the concurrence of high tides and waves.

Overtopping estimates are sensitive to errors in beach geometry and significant wave height. RTK surveys immediately before potential flooding events would minimize geometry errors whereas significant wave height estimates would benefit from in-situ observation or validated wave transformation models for a given area. Parameterization of empirical overtopping models at the slope toe is inconsistent with many natural beaches, empirical models that rely on breaker height may be more suitable for natural beach runup and overtopping. Comprehensive field observations of wave runup, overtopping and coastal flooding are required to develop, improve and validate coastal flood predictions.

BreZo is found to be a robust shallow-water solver in this study, but we expect that other numerical models could offer a similar level of performance. From a numerical perspective, the model should account for

Table 3
Hydrodynamic urban drainage and flood defense results summary.

Figure	Drain	Wall	Berm	A (km ²)	h _{avg} (cm)	h _{se}
6a	As reported	Yes	No	0.082	12.2	75
6b	No drainage	Yes	No	0.105	14.6	102
6c	All drains	Yes	No	0.075	11.0	-0
-	As reported	No	No	0.070	9.1	52
-	As reported	+ 30 cm	No	0.082	12.2	80
7	As reported	No	No	0.088	11.7	53
7	As reported	+ 30 CM	No	0.119	14.0	110
8	As reported	Yes	Yes	0.022	9.0	0

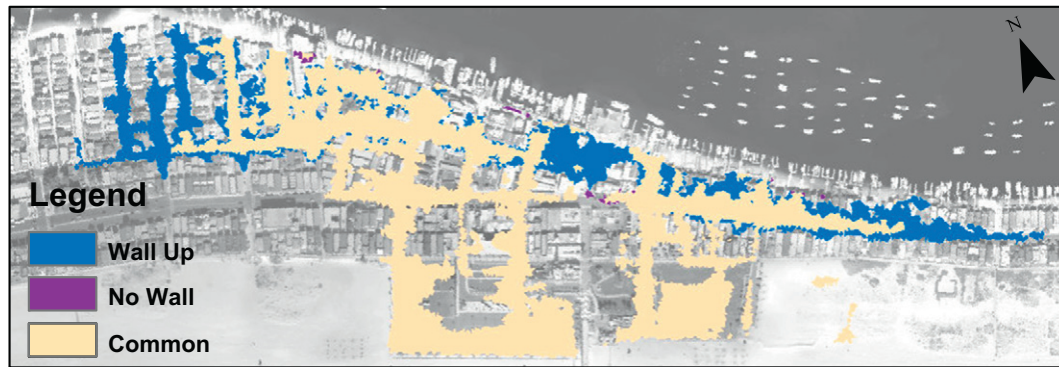


Fig. 7. Wall results. Beige shows the common flood extent for no wall and wall simulations with an additional 30 cm of water level. Purple shows the additional area flooded with the wall removed (flooded area increases slightly along the bayside) and blue represents the additional area predicted to flood if the wall is raised 30 cm.

wetting and drying without mass conservation errors or stability problems, allow for precise depiction of urban terrain, be amenable to general purpose sources and sinks to account for overtopping flows and drainage effects, and should be computationally efficient. Hydrodynamic models such as this one are recommended as the basis for flood risk management in defended urban terrain. Static or ‘bathtub’ models should be avoided as these fail to account for the critical temporal dynamics, drainage and flood defense infrastructure.

5. Conclusions

This study presents a new paradigm in urban coastal flood prediction: flood impacts at the parcel scale are predicted by embedding an empirical wave overtopping model within a two-dimensional shallow-water model that accounts for embayment dynamics, overland flow, weir-like overtopping of concrete flood walls, and drainage into the storm water system. Three-dimensional, non-hydrostatic wave effects are parameterized while two-dimensional hydrostatic flows are resolved. Two empirical wave overtopping models were used to estimate temporally variable overtopping flows, HR and Eurotop, and represent substantial improvements over static methods.

Urban drainage, flood defense walls, and beach berms significantly alter flooding outcomes. If the drainage system is functional, i.e., water levels are below the threshold of storm drain closure so that water can

exhaust to the bay, flooded area and depth are substantially reduced. Flood defense may constrain overtopping volume and, exclusion of walls decreased flooded areas whereas elevated walls increased flood water retention. Paradoxically, attempts to minimize one flooding mechanism (i.e., tidal or high embayment water level) may exacerbate an alternative flooding mechanism (i.e., beach overtopping). In this case, temporary measures were effective in protecting the backshore from flooding and resolving this temporarily altered berm crest elevation within the overtopping models fundamentally changed the flooding outcomes. These findings suggest that both permanent and temporary flood abatement measures deserve careful consideration. Temporary measures such as cautionary sandbagging, storm system dewatering and beach scraping activities should be thoroughly investigated for efficacy as potential sea level rise adaptation measures.

Although this study benefits from unique observational data, a paucity of available validation data has principally obstructed urban coastal flood prediction. High sensitivity to flood defense infrastructure for both weir-like overflow and wave overtopping necessitates high resolution, high accuracy infrastructure and observational datasets. Information regarding drain locations and capacity, flood defense elevations, wall condition, and temporary flood procedures should be rigorously documented. When possible, flooding events should be observed with high accuracy RTK surveys and time series of flood water levels at various locations. Additionally, quantitative data should be supported by

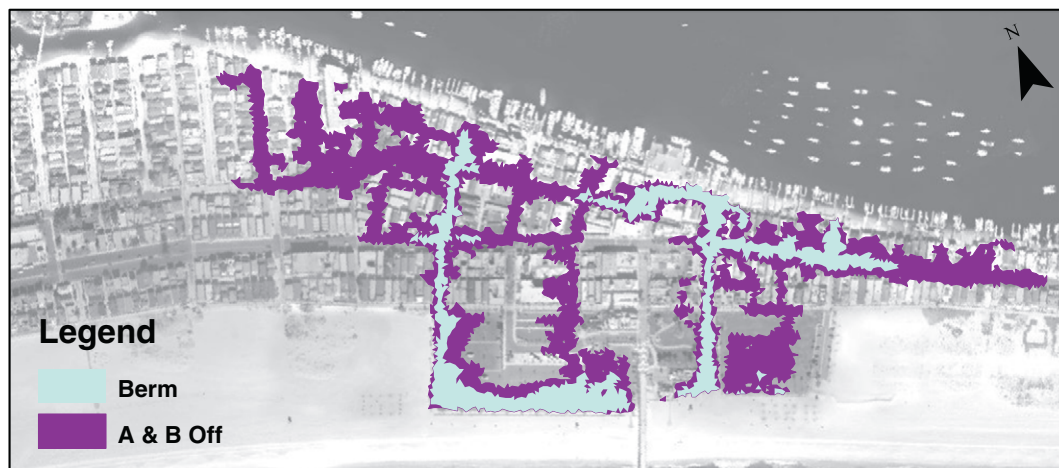


Fig. 8. Flood prediction with temporary scraped berm added (light blue) and without (purple).

qualitative validation data such as photographs and post-flood interviews or surveys. These datasets will serve to advance crucial predictive urban coastal flood models.

Acknowledgments

This work was supported by the California Department of Boating and Waterways, the Infrastructure Management and Extreme Events program of the National Science Foundation (CMMI-1129730), the Newkirk Center for Science and Society and the Robert L. Wiegel Scholarship and was made possible by the gracious cooperation of the City of Newport Beach personnel who shared geospatial data, photographs, and invaluable site-specific knowledge. The authors would like to specifically acknowledge Maria Reis and Terry Hedges for generously sharing details of their overtopping model, Sean Crosby for providing MEM CDIP wave spectra, and Bob Guza for the numerous helpful discussions. The author thanks the anonymous reviewers for their thoughtful and constructive comments.

References

- Ahrens, J.P., Heimbaugh, M.S., Davidson, D.D., 1986. Irregular wave overtopping of seawall/revetment configurations, Roughans Point, Massachusetts, USA. Final Report of Experimental Model Investigation, Coastal Engineering Research Center, Department of the Army, Mississippi.
- Anselme, B., Durand, P., Thomas, Y.F., Nicolae-Lerma, A., 2011. Storm extreme levels and coastal flood hazards: a parametric approach on the French coast of Languedoc (district of Leucate). *Compt. Rendus Geosci.* 343, 677–690.
- Arega, F., Sanders, B.F., 2004. Dispersion model for tidal wetlands. *J. Hydraul. Eng. ASCE* 130 (8), 739–754.
- Bates, P.D., De Roo, A.P.J., 2000. A simple raster-based model for floodplain inundation simulation. *J. Hydrol.* 236, 54–77.
- Bates, P.D., Dawson, R.J., Hall, J.W., Horritt, M.S., Nicholls, R.J., Wicks, J., Hassan, M.A.A.M., 2005. Simplified two-dimensional numerical modelling of coastal flooding and example applications. *Coast. Eng.* 52 (9), 793–810.
- Battjes, J.A., Gerritsen, H., 2002. Coastal modelling for flood defence. *Phil. Trans. R. Soc. A* 360, 1461–1475.
- Begnudelli, L., Sanders, B.F., Bradford, S.F., 2008. Adaptive Godunov-based model for flood simulation. *J. Hydraul. Eng.* 134 (6), 714–725.
- Bernatchez, P., Fraser, C., Lefaivre, D., Dugas, S., 2011. Integrating anthropogenic factors, geomorphological indicators and local knowledge in the analysis of coastal flooding and erosion hazards. *Ocean Coast. Manag.* 53, 621–632.
- Booij, N., Ris, R.C., Holthuijsen, L.H., 1999. A third-generation wave model for coastal regions: 1. Model description and validation. *J. Geophys. Res. Oceans Atmos.* 104 (C4), 7649–7666 (19782012).
- Brown, J.D., Spencer, T., Moeller, I., 2007. Modeling storm surge flooding of an urban area with particular reference to modeling uncertainties: a case study of Canvey Island, United Kingdom. *Water Resour. Res.* 43 (W06402). <http://dx.doi.org/10.1029/2005WR004597>.
- CBS, 2011. High Tide, Surf Cause Flooding in Newport Beach. CBS Los Angeles, aired August, 31, 2011. Available online at <http://losangeles.cbslocal.com/2011/08/31/high-tide-surf-cause-flooding-in-newport-beach/>.
- CDIP, P. The Coastal Data Information Program, Scripps Institution of Oceanography <http://cdip.ucsd.edu/>.
- Cea, L., French, J.R., Vazquez-Cendon, M.E., 2006. Numerical modelling of tidal flows in complex estuaries including turbulence: an unstructured finite volume solver and experimental validation. *Int. J. Numer. Methods Eng.* 67, 1909–1932.
- Cheung, K.F., Phadke, A.C., Wei, Y., Rojas, R., Douyere, Y.J.M., Martino, C.D., Houston, S.H., Liu, P.L.F., Lynett, P.J., Dodd, N., Liao, S., Nakazaki, E., 2003. Modeling of storm induced coastal flooding for emergency management. *Ocean Eng.* 30, 1353–1386.
- Chini, N., Stansby, P.K., 2012. Extreme values of coastal wave overtopping accounting for climate change and sea level rise. *Coast. Eng.* 65, 27–37.
- Church, J.A., Clark, P.U., Cazenave, A., Gregory, J.M., Jevrejeva, S., Levermann, A., Merrifield, M.A., Milne, G.A., Nerem, R.S., Nunn, P.D., Payne, A.J., Pfeffer, W.T., Stammer, D., Unnikrishnan, A.S., 2013. Sea level change. In: Stocker, T.F., Qin, D., Plattner, G.-K., Tignor, M., Allen, S.K., Boschung, J., Nauels, A., Xia, Y., Bex, V., Midgley, P.M. (Eds.), *Climate Change 2013: The Physical Science Basis. Contribution of Working Group I to the Fifth Assessment Report of the Intergovernmental Panel on Climate Change*. Cambridge University Press, Cambridge, United Kingdom and New York, NY, USA.
- Coveney, S., Fotheringham, A.S., 2011. The impact of DEM data source on prediction of flooding and erosion risk due to sea-level rise. *Int. J. Geogr. Inf. Sci.* 25 (7), 1191–1211.
- Dawson, R.J., Dickson, M.E., Nicholls, R.J., Hall, J.W., Walkden, M.J.A., Stansby, P., Mokrech, M., Richards, J., Zhou, J., Milligan, J., Jordan, A., Pearson, S., Rees, J., Bates, P., Koukoulas, S., Watkinson, A., 2009. Integrated analysis of risks of coastal flooding and cliff erosion under scenarios of long term change. *Clim. Chang.* 95 (1–2), 249–288.
- Federal Emergency Management Agency (FEMA), 2004. Guidelines and Specifications for Flood Hazard Mapping Partners Appendix D. Final Draft Guidelines for Coastal Flood Hazard Analysis and Mapping for the Pacific Coast of the United States. Available online at <http://www.fema.gov/library/viewRecord.do?id=2188>.
- Fewtrell, T.J., Bates, P.D., Horitt, M., Hunter, N.M., 2008. Evaluating the effect of scale in flood inundation modelling in urban environments. *Hydrol. Process.* 22, 5107–5118.
- Fewtrell, T.J., Duncan, A., Sampson, C.C., Neal, J.C., Bates, P.D., 2011. Benchmarking urban flood models of varying complexity and scale using high resolution terrestrial LiDAR data. *Phys. Chem. Earth* 36 (7–8), 281–291.
- Gallegos, H.A., Schubert, J.E., Sanders, B.F., 2009. Two-dimensional, high-resolution modeling of urban dam-break flooding: a case study of Baldwin Hills, California. *Adv. Water Resour.* 32, 1323–1335.
- Gallien, T.W., Schubert, J.E., Sanders, B.F., 2011. Predicting tidal flooding of urbanized embayments: a modeling framework and data requirements. *Coast. Eng.* 58 (6), 567–577.
- Gallien, T.W., Barnard, P.L., van Ormondt, M., Foxgrover, A.C., Sanders, B.F., 2013. A parcel-scale coastal flood forecasting prototype for a Southern California urbanized embayment. *J. Coast. Res.* 29 (3), 642–656.
- Gesch, D.B., 2009. Analysis of Lidar elevation data for improved identification and delineation of lands vulnerable to sea-level rise. *J. Coast. Res.* 25 (6), 49–58.
- Guinot, V., 2003. *Godunov-Type Schemes*. Elsevier, Amsterdam.
- Heberger, M., Cooley, H., Herrera, P., Gleick, P.H., Moore, E., 2009. The Impacts of Sea-Level Rise on the California Coast. California Climate Change Center, Sacramento.
- Hedges, T.S., Reis, M.T., 1998. Random wave overtopping of simple seawalls a new regression model. *Water Marit. Energy J.* 157, 113–122.
- Hu, K., Mingham, C.G., Causon, D.M., 2000. Numerical simulation of wave overtopping of coastal structures using the non-linear shallow water equations. *Coast. Eng.* 41, 433–465.
- Hubbard, M.E., Dodd, N., 2002. A 2D numerical model of wave run-up and overtopping. *Coast. Eng.* 47, 1–26.
- Hunt, I.A., 1959. Design of seawalls and breakwaters. *J. Waterw. Harb. Div.* 85, 123–125/2152.
- Hunt, J.C.R., 2005. Inland and coastal flooding: developments in prediction and prevention. *Phil. Trans. R. Soc. A* 363, 1475–1491.
- Kirshen, P., Kneel, K., Ruth, M., 2008. Climate change and coastal flooding in Metro Boston: impacts and adaptation strategies. *Clim. Chang.* 90, 453–473.
- Knowles, N., 2009. Potential Inundation due to Rising Sea Levels in the San Francisco Bay Region. California Climate Change Center, Sacramento.
- Laudier, N.A., Thorntorn, E.B., MacMahan, J., 2011. Measured and modeled wave overtopping on a natural beach. *Coast. Eng.* 58, 815–825.
- Liu, P.L.F., Lin, P., Chang, K.A., Sakakiyama, T., 1999. Numerical modelling of wave interaction with porous structures. *J. Waterw. Port Coast. Ocean Eng.* 125 (6), 322–330.
- Losada, I.J., Lara, J.L., Gunache, R., Gonzalez-Ondina, J.M., 2008. Numerical analysis of wave overtopping of rubble mound breakwaters. *Coast. Eng.* 55, 47–62.
- Lynett, P.J., Melby, J.A., Kim, D.H., 2010. An application of Boussinesq modeling to hurricane wave overtopping and inundation. *Ocean Eng.* 37 (1), 135–153.
- Martinelli, L., Zanuttigh, B., Corbau, C., 2010. Assessment of coastal flooding hazard along the Emilia Romagna littoral, IT. *Coast. Eng.* 57, 1042–1058.
- Mase, H., Reis, T.S., Shareef, M., Nagahashi, S., 2003. Wave overtopping formula for gentle slopes incorporating wave run up. *Proc. of Coastal Engineering, JSCE*, 50, pp. 636–640.
- Mignot, E., Paquier, A., Haider, S., 2006. Modeling floods in dense urban area using 2D shallow water equations. *J. Hydrol.* 327, 186–199.
- National Oceanic and Atmospheric Administration (NOAA), 2012. NOAA Tides and Currents. Available at <http://tidesandcurrents.noaa.gov/>.
- National Research Council, 2009. Mapping the Zone: Improving Flood Map Accuracy. The National Academies Press, Washington, DC.
- Néelz, S., Pender, G., Villaneuva, I., Wilson, M., Wright, N.G., Bates, P.D., Mason, D., Whitlow, C., 2006. Using remotely sensed data to support flood modelling. *Water Manag.* 159 (1), 35–43.
- Okayasu, A., Suzuki, T., Matsubayashi, Y., 2005. Laboratory experiment and three-dimensional large eddy simulation of wave overtopping on gentle slope seawalls. *Coast. Eng.* 47, 71–89.
- Orange County Environmental Management Agency, 1996. Orange County Local Drainage Manual. Retrieved from http://www.ocflood.com/docs_online_manuals.aspx.
- Owen, M.W., 1980. Design of seawalls allowing for wave overtopping. Report No. EX 924, HR Wallingford, United Kingdom.
- Poulter, B., Halpin, P.N., 2008. Raster modelling of coastal flooding from sea-level rise. *Int. J. Geogr. Inf. Sci.* 22 (2), 167–182.
- Pullen, T., Allsop, N.W.H., Bruce, T., Kortenhaus, A., Schüttrumpf, H., Van der Meer, J.W., 2007. EurOtop: wave overtopping of sea defences and related structures: Assessment manual. Available at <http://www.overtopping-manual.com/manual.html>.
- Purvis, M.J., Bates, P.D., Hayes, C.M., 2008. A probabilistic methodology to simulate future coastal flood risk due to sea level rise. *Coast. Eng.* 55, 1062–1073.
- Reeve, D.E., Soliman, A., Lin, P.Z., 2008. Numerical study of combined overflow and wave overtopping over a smooth impermeable seawall. *Coast. Eng.* 55, 155–166.
- Reis, M.T., Hu, K., Hedges, T.S., Mase, H., 2008. A comparison of empirical, semiempirical and numerical wave overtopping models. *J. Coast. Res.* 24, 250–262.
- Sampson, C.C., Fewtrell, T.J., Duncan, A., Shaad, K., Horritt, M.S., Bates, P.D., 2012. Use of terrestrial laser scanning data to drive decimetric resolution urban inundation models. *Adv. Water Resour.* 41, 1–17.
- Sanders, B.F., 2008. Integration of a shallow-water model with a local time step. *J. Hydraul. Res.* 46 (8), 466–475.
- Schubert, J.E., Sanders, B.F., 2012. Building treatments for urban flood inundation models and implications for predictive skill and modeling efficiency. *Adv. Water Resour.* 41, 49–64.
- Schubert, J.E., Sanders, B.F., Smith, M.J., Wright, N.G., 2008. Unstructured mesh generation and landcover-based resistance for hydrodynamic modeling of urban flooding. *Adv. Water Resour.* 31 (12), 1603–1621.
- Schubert, J.E., Gallien, T.W., Shakeri Majd, M., Sanders, B.F., 2014. Terrestrial laser scanning of anthropogenic beach berm erosion and overtopping. *J. Coast. Res.* <http://dx.doi.org/10.2112/JCOASTRES-D-14-00037.1> (in press).

- Shewchuk, J.R., 1996. Triangle: engineering a 2D quality mesh generator and Delaunay triangulator. In: Lin, M.C., Manocha, D. (Eds.), *Applied Computational Geometry: Towards Geometric Engineering*. Lecture Notes in Computer Science, vol. 1148. Springer-Verlag, pp. 203–222 (Software: <<http://www-2.cs.cmu.edu/~quake/triangle.html>>).
- Smith, R.A.E., Bates, P.D., Hayes, C., 2012. Evaluation of a coastal flood inundation model using hard and soft data. *Environ. Model. Softw.* 30, 35–46.
- Southern California Beach Process Study (SCBPS), 2014. LiDAR Metadata. Available at <http://www.csc.noaa.gov/digitalcoast/data/coastallidar/index.html>.
- State of California, 2010. State of California Sea-Level Rise Interim Guidance Document (October).
- Stockdon, H.F., Holman, R.A., Howd, P.A., Sallenger, A.H., 2006. Empirical parameterization of setup, swash and runup. *Coast. Eng.* 53, 573–588.
- Strauss, B.H., Ziemiński, R., Weiss, J.L., Overpeck, J.T., 2012. Tidally adjusted estimates of topographic vulnerability to sea level rise and flooding for the contiguous United States. *Environ. Res. Lett.* 7 (12 pp.).
- Sturm, T.W., 2001. *Open Channel Hydraulics*. McGraw Hill, Boston, MA.
- TAW, 2002. Technical Report Wave Run-Up and Wave Overtopping at Dikes. Technical Advisory Committee on Flood Defence, The Netherlands.
- Taylor, Peter J., 1977. *Quantitative Methods in Geography: An Introduction to Spatial Analysis*. Houghton Mifflin Harcourt, Boston, Massachusetts (396 pp.).
- Tebaldi, C., Strauss, B.H., Zervas, C.E., 2012. Modelling sea level rise impacts on storm surges along US coasts. *Environ. Res. Lett.* 7, 11.
- Thomalla, F., Brown, J., Kelman, I., Möller, I., Spence, R., Spencer, T., 2002. Towards an integrated approach for coastal flood impact assessment. *Proceedings of the Solutions to Coastal Disasters Conference, ASCE*, pp. 142–158.
- Toro, E.F., 2001. *Shock-Capturing Methods for Free-Surface Shallow Flows*. Wiley, Chichester, U.K.
- U.S. Army Corps of Engineers (USACE), 1984. *Shore Protection Manual*. Coastal Engineering Research Center, Vicksburg, MI.
- U.S. Army Corps of Engineers (USACE), 2002. *Coast of California Storm and Tidal Waves Study South Coastal Region*. Orange County, Los Angeles District, Los Angeles, CA.
- Villaneueva, I., Wright, N.G., 2006. Linking Riemann and storage cell methods for flood predictions. *Proc. Inst. Civ. Eng. Water Manag.* 159 (1), 27–33.
- Villatoro, M., Silva, R., Méndez, F.J., Zanuttigh, B., Pan, S., Trifonova, E., Losada, I.J., Izaguirre, C., Simmonds, D., Reeve, D.E., Mendoza, E., Martinelli, L., Formentin, S.M., Galiatsatou, P., Eftimova, P., 2014. An approach to assess flooding and erosion risk for open beaches in a changing climate. *Coast. Eng.* 87, 50–76.
- Wadey, M.P., Nicholls, R.J., Hutton, C., 2012. Coastal flooding in the solent: an integrated analysis of defences and inundation. *Water* 4, 430–459.
- Webster, T.L., Forbes, D.L., Dickie, S., Shreenan, R., 2004. Flood-risk mapping for storm-surge events and sea-level rise using LiDAR for southeast New Brunswick. *Can. J. Remote. Sens.* 32 (3), 194–211.
- Yin, J., Yin, Z., Hu, X., Xu, S., Wang, J., Li, Z., Zhong, H., Gan, F., 2011. Multiple scenario analyses forecasting the confounding impacts of sea level rise and tides from storm induced coastal flooding in the city of Shanghai, China. *Environ. Earth Sci.* 63, 407–414.